Supporting Information

Polyhydroxy Starch with Abundant Hydroxyl and Unique Structure Enables Uniform Zn Deposition

Ming Song,‡[a] Zhaohe Guo,‡[a] Yan Xu,*[a] Xueyao Mo,[a] Xuena Xu,[b] Limei Sun,[a] Wenyi Tan,[a] Dongliang Chao[c] and Wanhai Zhou*[c]

[a] School of Materials and Chemical Engineering, Xuzhou University of Technology, Xuzhou 221018, China
[b] Department of Mechanical Engineering，Tsinghua University，Beijing 100084，China
[c] Laboratory of Advanced Materials, Shanghai Key Laboratory of Molecular Catalysis and Innovative Materials, Fudan University, Shanghai, 200433, China

*Correspondence:
xuyan8787@163.com (Y.X), zhouwh@fudan.edu.cn (W.Z.)

Experimental

Materials

Zinc sulfate heptahydrate ($ZnSO_4 \cdot 7H_2O$, 99%), starch ($(C_6H_{10}O_5)n$), N-Methyl-2-pyrrolidone (NMP, C_5H_9NO, 99%), Oxalic acid ($H_2C_2O_4$, 99%) and Vanadium pentoxide (V_2O_5, 99%) were purchased from Aladdin. Polyvinylidene fluoride (PVDF, Arkema) and conductive carbon black (Timical) were purchased from Saibo Electrochemical Materials Pte Ltd. Glass microfiber filter (Whatman GF/D, Diameter 47mm, 1823-047) was obtained from Huidi Pte Ltd. Zn foils (30 μm, 99.9%), Cu foil (30 μm, 99.9%), Titanium mesh and stainless steel were provided by Shengshida Metallic Materials Pte Ltd.

Electrolyte preparation

The 1 M $ZnSO_4$ aqueous electrolyte was prepared using $ZnSO_4 \cdot 7H_2O$ and deionized water based on the molar ratio. Certain amount of starch was introduced into the $ZnSO_4$ electrolyte to obtain the electrolyte containing different amounts of starch. The electrolyte without starch was denoted as "without starch", and the electrolyte with 0.2 mg/mL starch was signed as "with starch". The electrolyte with 0.1 and 0.4 mg mL^{-1} starch were denoted as 0.1 starch and 0.4 starch, respectively.

Fabrication of Zn||Zn and Zn||Cu cell

The Zn plating/stripping tests were performed on Zn symmetrical cells. Two pieces of Zn foil were used as electrodes for Zn||Zn cell. The GE-Whatman glass fiber was employed as the separator. Coulombic efficiency (CE) measurements were carried out on asymmetrical Zn||Cu cells. Zn foil and copper foil were used as electrodes. The electrolyte and glass fiber in Zn||Cu cell were the same as that in Zn||Zn cell.

Fabrication of Zn||VO_2 full Cell

VO_2 was synthesized by the hydrothermal method. Typically, 1.2 g of V_2O_5 was dispersed in 40 mL of deionized water under string, followed by adding 1.8 g of $H_2C_2O_4$. Then, the above suspension was heated at 80 °C for 1 h. After that, the solution was transformed into a hydrothermal reactor, and maintained at 180 °C for 4 h. When the reactor cooled down to room temperature, the product was washed with deionized water for several times to obtain the VO_2. The cathode was prepared by mixing VO_2 with conductive carbon black and PVDF at the weight ratio of 7:2:1 and dissolving the above mixture in an appropriate amount of NMP to form homogeneous slurry. The obtained slurry was then spread onto the titanium mesh, and dried in a vacuum oven at 60 °C overnight. The mass loading of the above cathode active materials was about 2.0~4.0 mg cm^{-2}. Zinc foil and glass fiber were used as the anode and separator, respectively.

Electrochemical Test

The performances of Zn||Zn symmetric cells, Zn||Cu asymmetric cells, and Zn||VO_2 full cells were carried out on a Neware CT-3008 battery test system. The Zn||Zn cells were tested at 5 mA cm^{-2} / 1 mAh cm^{-2}, 5 mA cm^{-2} / 5 mAh cm^{-2}, 10 mA cm^{-2} / 5 mAh cm^{-2}, and 30 mA cm^{-2} / 1 mAh cm^{-2} respectively. The rate performance of Zn||Zn

cells were tested at 1, 2, 3, 5, 10, 20, 30, 40 and 1 mA cm^{-2} with the areal capacity of 1 mAh cm^{-2}. The Zn||Cu asymmetric cells were carried out at 1 mA cm^{-2} / 0.5 mAh cm^{-2}. For Zn||VO_2 cell, the rate performance was tested at various current densities (0.1, 0.2, 0.5, 1, and 2 A g^{-1}) and the cycling performance was evaluated with the voltage range of 0.3~1.5 V under 0.5 A g^{-1}. The specific capacities were evaluated according to the mass of active materials. The corrosion, diffusion, and hydrogen evolution behaviors of Zn foil anode were tested under an electrochemical workstation (CHI 660e) with a three-electrode system (Zn foil as work electrode, Pt as counter electrode, and Ag/AgCl as reference electrode). The Tafel plot was recorded with a potential range of ±0.3 V versus open-circle potential of the system at a scan rate of 1 mV s^{-1}. The hydrogen evolution performance was collected by linear sweep voltammetry (LSV) with a potential range of -1~-1.6 V at a scan rate of 1 mV s^{-1}. The diffusion curves were measured by chronoamperometry method under an overpotential of -150 mV. The cyclic voltammetry (CV) for the nucleation overpotential was tested with a voltage rage of -1.4~-0.2 at a scan rate of 1 mV s^{-1} (Zn foil as counter electrode, Ti as work electrode, and Ag/AgCl as reference electrode). The electrochemcial potential window was tested at 1 mV s^{-1} (steel-mesh as working electrode and counter electrode, and Ag/AgCl electrode as reference electrode). Electrochemical impedance spectroscopy (EIS) was implemented within a range of 10^5 to 10^{-2} Hz.

Characterization

The properties of electrolyte were studied by FT-IR (Bruker Alfar) and contact angle meter (Jinhe, JY-PHB). The Zn foil (pristine, soaked and cycled) and VO_2 were characterized by the X-ray diffraction with Cu Kα (λ=1.54060 Å) (XRD, Rigaku, Ultima IV) and field-emission scanning electron microscopy (SEM, Hitachi SU8600). The cycled Zn electrolyte was also characterized by the X-ray photoelectron spectroscopy with Al kα ray (hv=1486.6eV) (XPS, ThermoFischer，ESCALAB 250XI). The images of Zn deposition process were obtained on an industrial optical microscope (Aoweisi, AW33T-4K). Morphology of zinc deposits plating on Cu foil at 20 mA cm^{-2} and 1 mAh cm^{-2} and the residual zinc deposits after stripping is characterized by SEM.

Electrochemical digital holography

The measurement was carried out in symmetric cells with bare Zn anodes as counter electrodes and various modified Zn anodes as working electrodes. 1M $ZnSO_4$ was selected as an electrolyte. A Mach-Zehnder interferometer optical setup was employed for electrochemical digital holography with a charge-coupled device camera to document the dynamic processes. During deposition/dissolution processes, the concentration of certain species in the solution can alter, which can be described as follows:

$$\Delta C = k\Delta n = k(\frac{\lambda_0}{2\pi d})\Delta\phi$$

where ΔC represents the change in the solution concentration. k refers to the concentrative refractivity. Δn is the change of the solution refractive index. λ_0 refers to the wavelength of the laser light. d is the path length of the refractive index change. Δϕ refers to the phase difference. The relationship between ΔC, Δϕ and the colours in the phase diagram is described below:

If Δϕ = 0, ΔC = 0, the phase map is green, indicating the concentration is unchanged;

If Δϕ < 0, ΔC < 0, the phase map is blue, indicating the concentration decreases;

If $\Delta\phi > 0$, $\Delta C > 0$, the phase map is yellow or red, indicating the concentration increases.

Calculations

The quantum chemistry calculations were carried out by using the Gaussian 09 software package. All structures were optimized from the density functional theory-based method using the B3LYP functional and the 6-31G basis set.

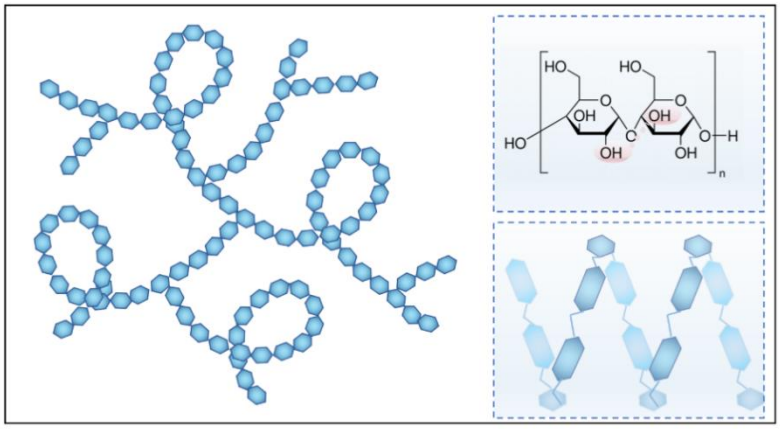

Fig. S1 Scheme of starch structure.

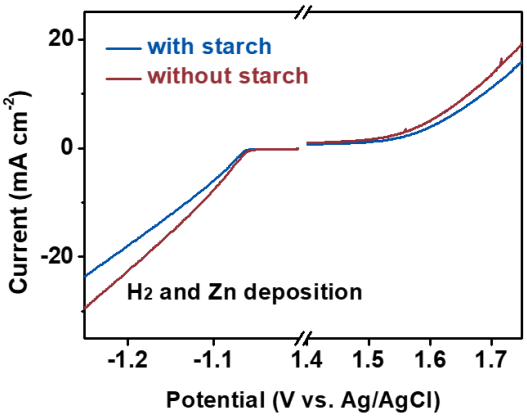

Fig. S2 The overall electrochemical stability window.

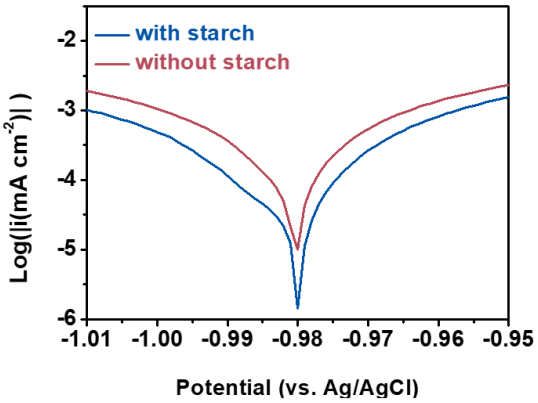

Fig. S3 Tafel curves in different electrolytes.

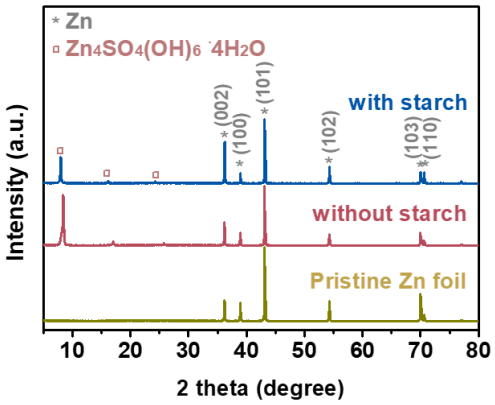

Fig. S4 XRD patterns of pristine Zn foil and Zn foil soaked in different electrolytes for 6 h.

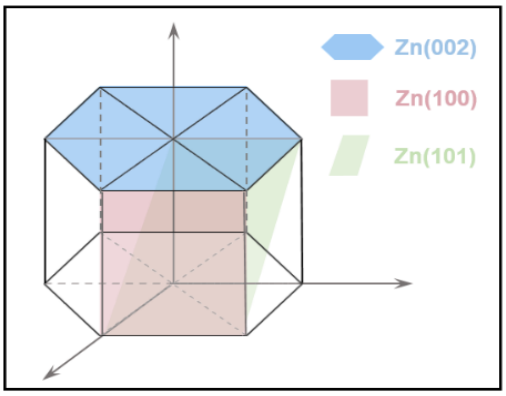

Fig. S5 Schematic diagram of different Zn planes.

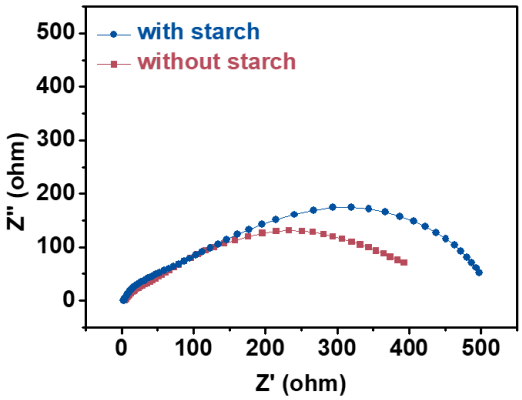

Fig. S6 EIS profile of Zn||Zn cells in different electrolytes after 10 cycles.

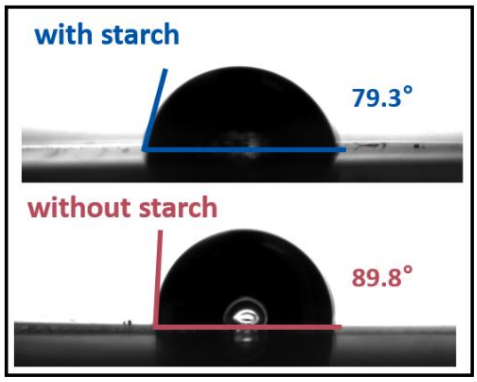

Fig. S7 Contact angles of different electrolytes on the Zn electrode.

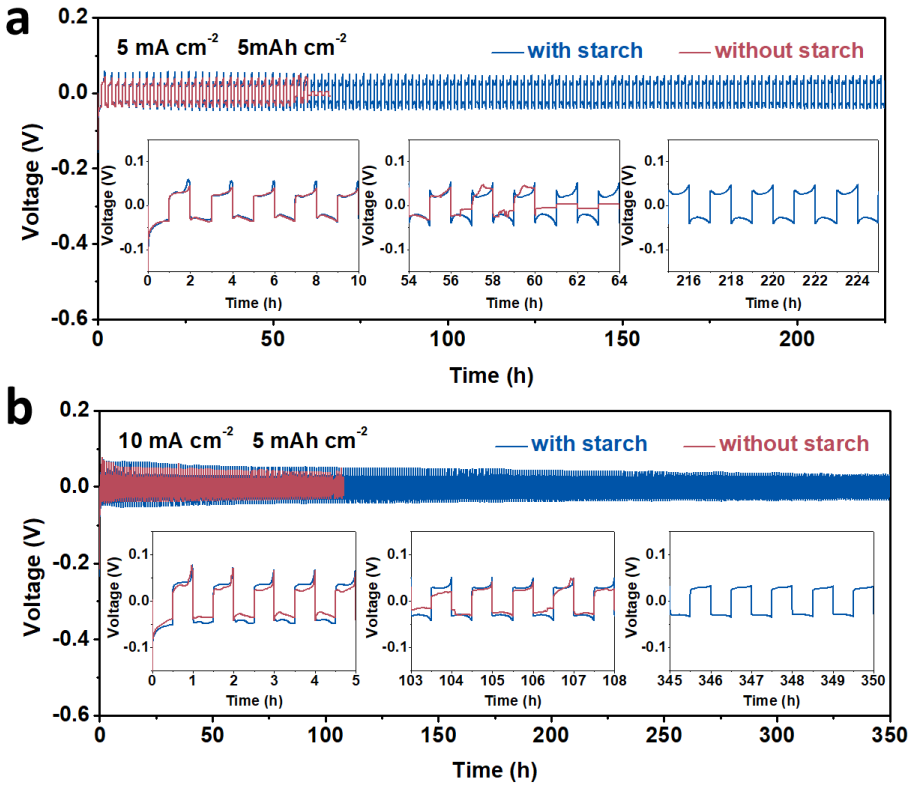

Fig. S8 Cycling performance of the Zn||Zn cells at (a) 5 mA cm^{-2} and 5 mAh cm^{-2}; (b) 10 mA cm^{-2} and 5 mAh cm^{-2}.

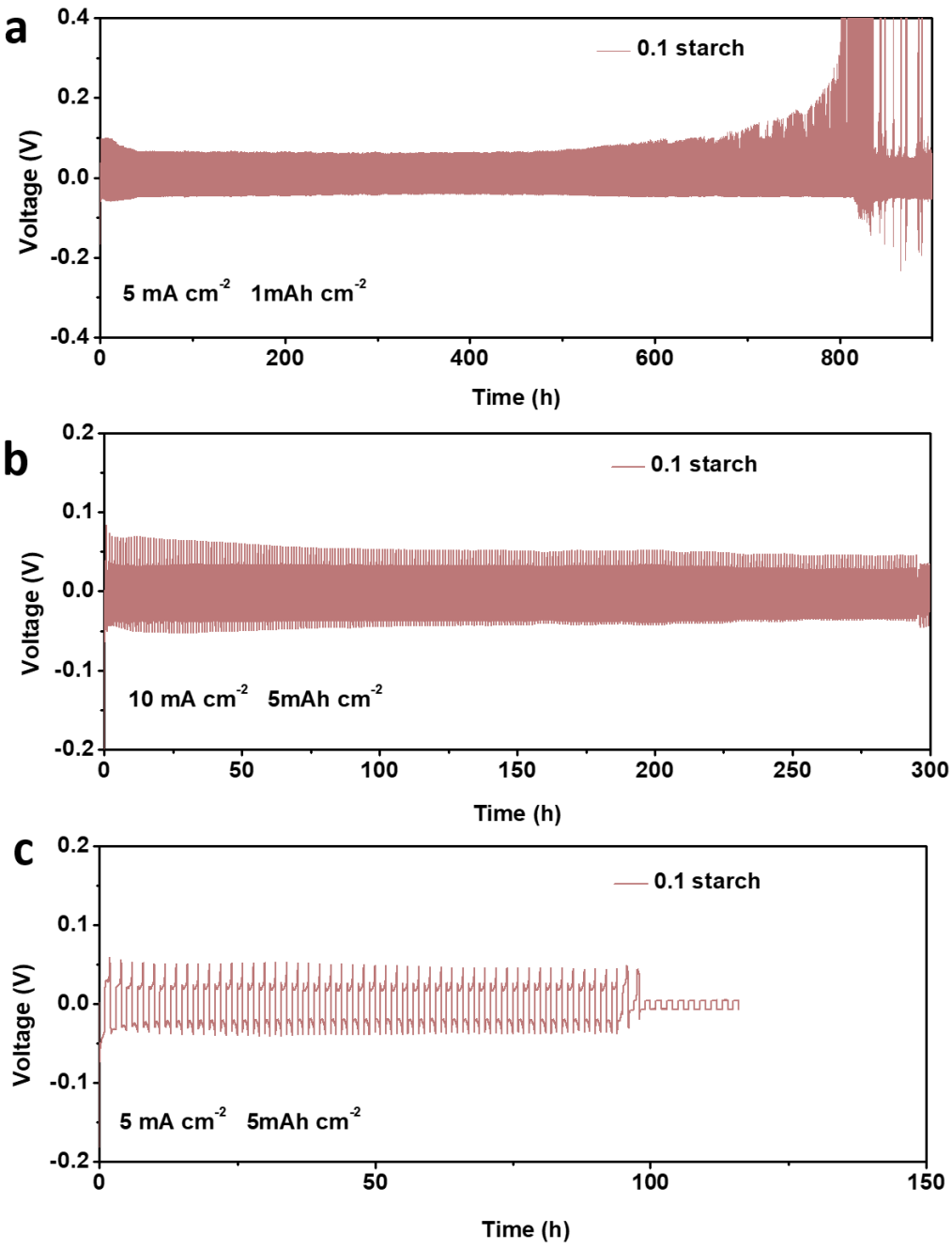

Fig. S9 Cycling performance of the Zn||Zn cells in electrolyte with 0.1 mg mL^{-1} starch at (a) 5 mA cm^{-2} / 1 mAh cm^{-2}; (b) 10 mA cm^{-2} /5 mAh cm^{-2}; (c) 5 mA cm^{-2}/5 mAh cm^{-2}.

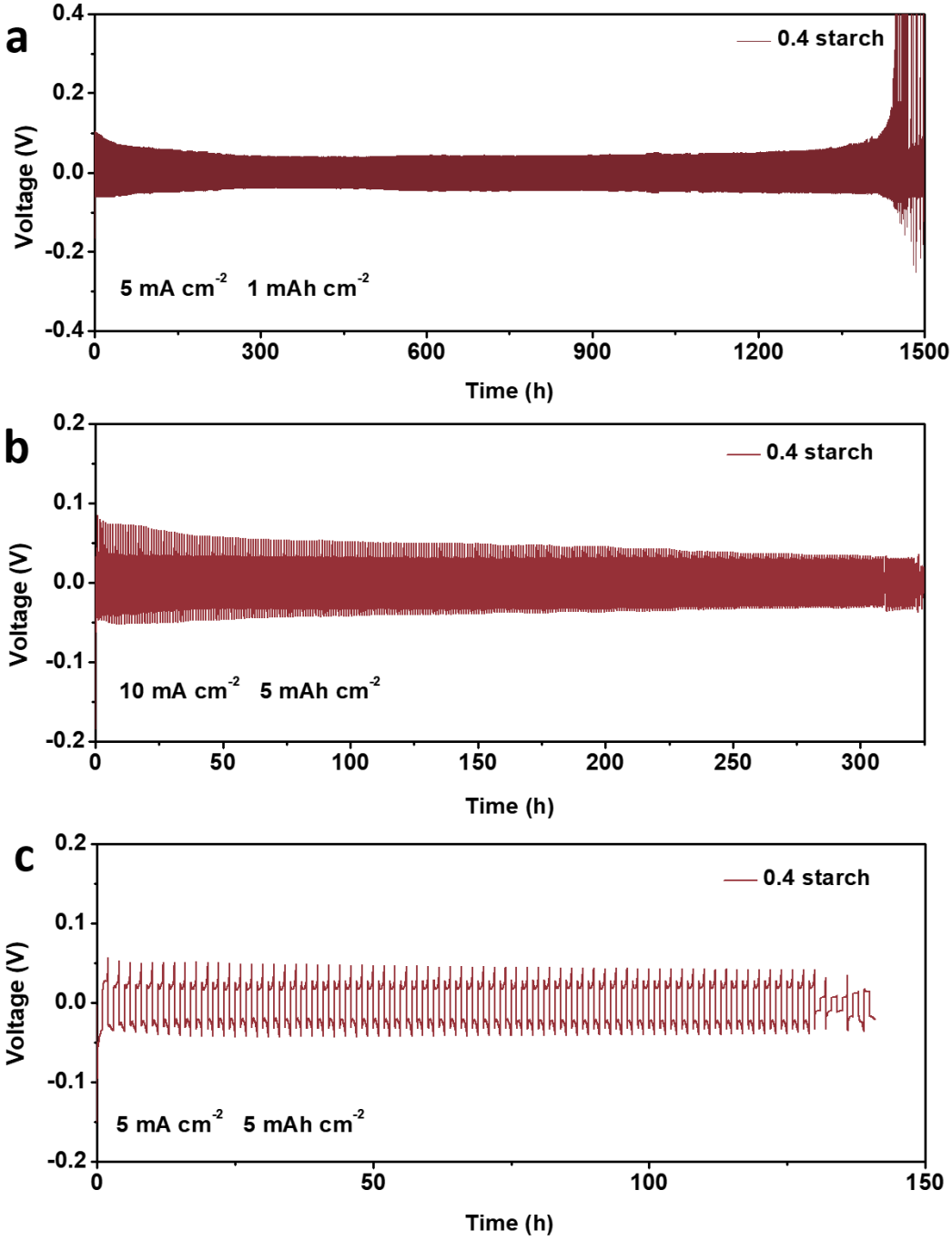

Fig. S10 Cycling performance of the Zn||Zn cells in electrolyte with 0.4 mg mL^{-1} starch at (a) 5 mA cm^{-2} / 1 mAh cm^{-2}; (b) 10 mA cm^{-2} /5 mAh cm^{-2}; (c) 5 mA cm^{-2}/5 mAh cm^{-2}.

Table S1 Summary of the performance of Zn||Zn cells in different electrolytes.

Electrolyte components	Current density (mA cm^{-2})	Areal capacity (mAh cm^{-2})	Lifespan (h)	Refs.
2 M $ZnSO_4$+1.5 wt% penta-sodium diethylene-triaminepentaacetic acid salt	2	1	800	1
2M $ZnSO_4$+10 M zinc dodecyltrimethyl ammonium chlorid	10	5	500	2
2 M $ZnSO_4$+100 mM trehalose	5	1	1600	3
2 M $ZnSO_4$+30 mM $TiOSO_4$	5	1	1000	4
2 M $ZnSO_4$+40 mM sodium L-tartrate	2	1	1500	5
2 M $ZnSO_4$+1 mM ammonium hydroxide	5	5	250	6
2 M $ZnSO_4$+2 mg mL^{-1} Tween-85	5	5	450	7
2 M ZnSO4+1% dioxane	10	3	180	8
2 M $ZnSO_4$+0.2 M sodium hydroxyethyl sulfonate	4	1	460	9
1 M $ZnSO_4$+1.0 mM epigallocatechin gallate	5	5	350	10
2 M $ZnSO_4$+1% dioxane	10	3	180	11
2 M $ZnSO_4$+1% fluorophosphate ester	5	1	1050	12
2 M $ZnSO_4$+0.25 g L^{-1} cellulose	5	1	600	13
2 M $ZnSO_4$+50 mM maltose	5	2.5	800	14
1 M $ZnSO_4$+0.2 mg mL^{-1} starch	5	5	250	This work
1 M $ZnSO_4$+0.2 mg mL^{-1} starch	5	1	1450	This work
1 M $ZnSO_4$+0.2 mg mL^{-1} starch	10	5	350	This work

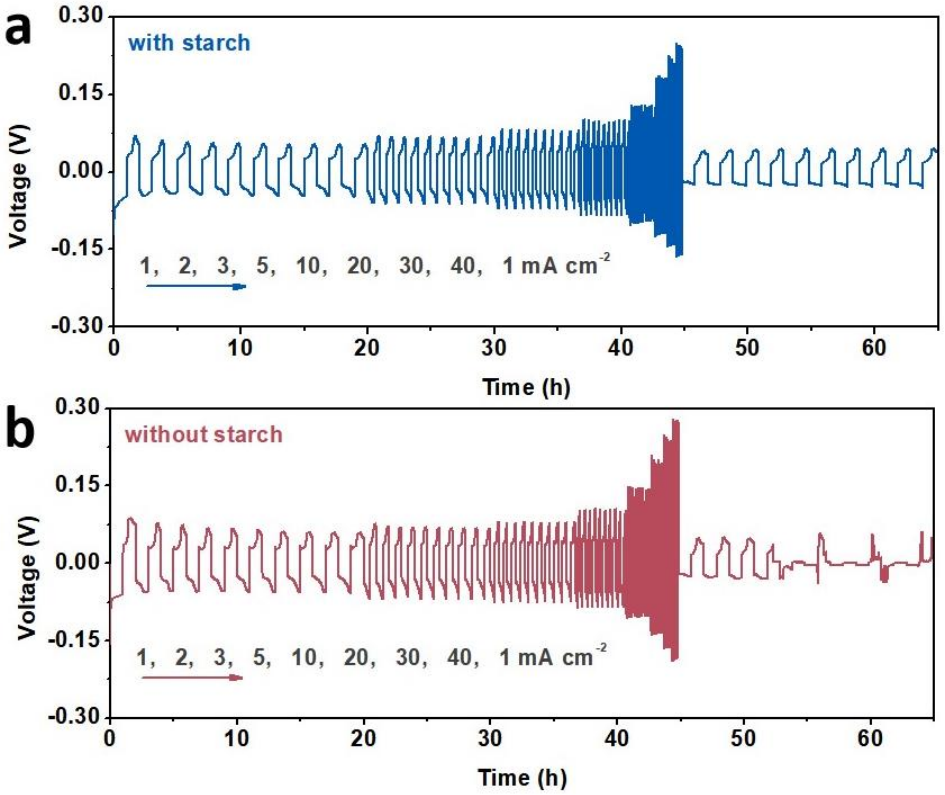

Fig. S11 Rate performance of Zn||Zn cells in different electrolytes.

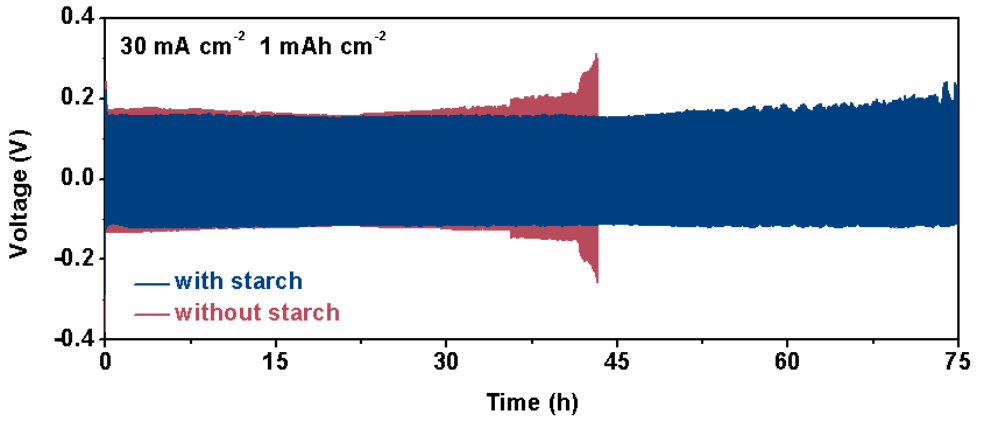

Fig. S12 Cycling performance of Zn||Zn cells in different electrolytes at 30 mA cm^{-2} and 1 mAh cm^{-2}.

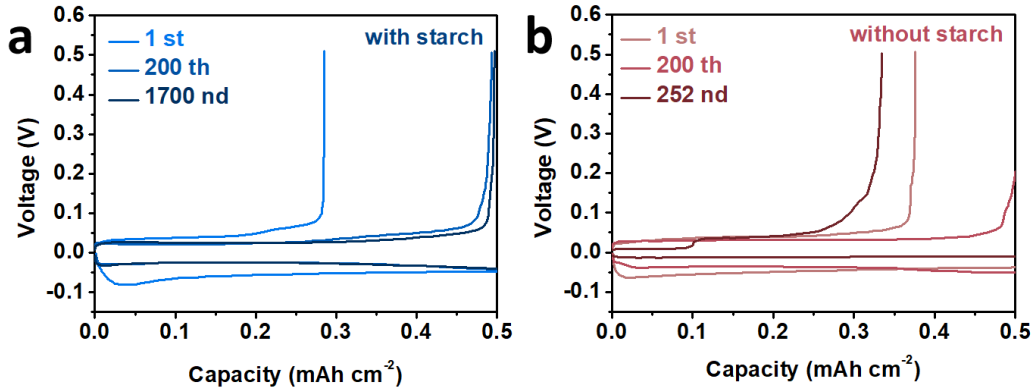

Fig. S13 Voltage and capacity of Zn||Cu cells at different cycles in electrolyte with (a) and without starch (b).

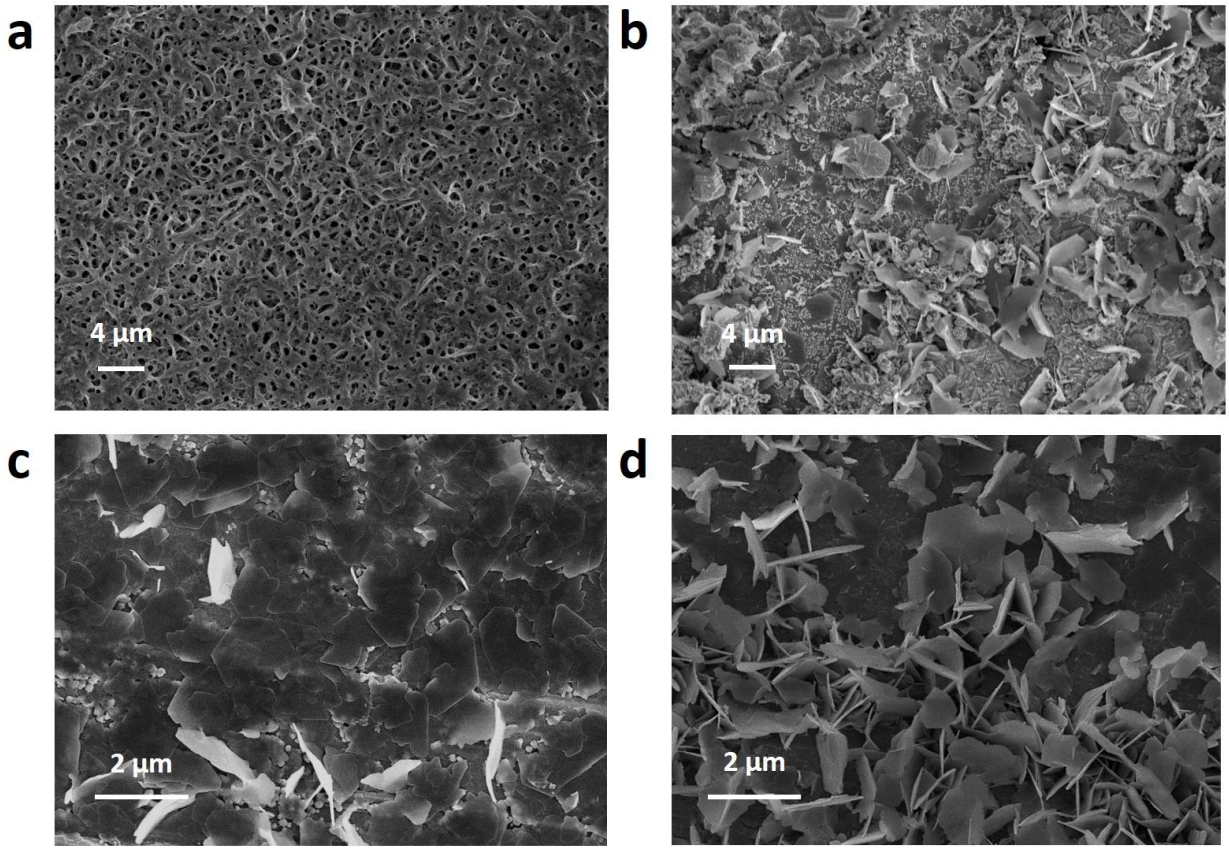

Fig. S14 Morphology of zinc deposits at 20 mA cm^{-2} and 1 mAh cm^{-2} in electrolyte (a) with starch; (b) without starch; Surface morphology of the copper foil after Zn stripping in electrolyte (c) with starch; (d) without starch.

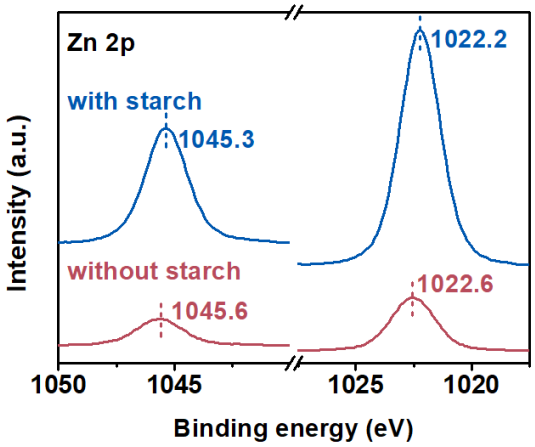

Fig. S15 XPS spectrum of Zn 2p after 50 cycles.

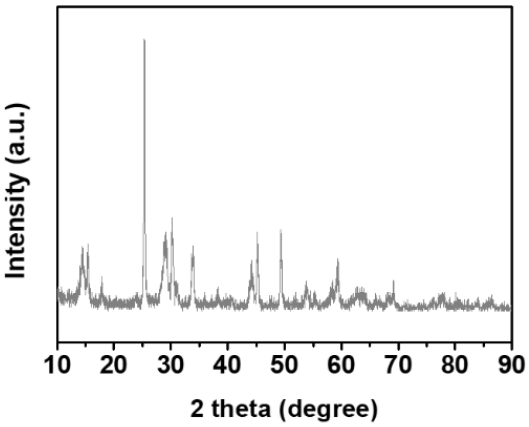

Fig. S16 XRD pattern of prepared VO_2.

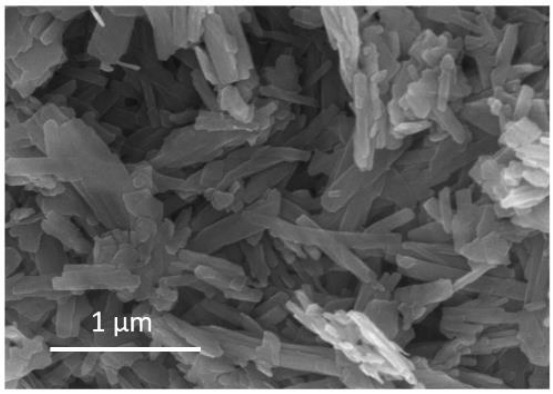

Fig. S17 SEM image of prepared VO_2.

Reference

[1] Y. Xia, R. Tong, J. Zhang, M. Xu, G. Shao, H. Wang, Y. Dong, C.A. Wang, *Nano-Micro Lett.*, 2024, **16**, 82.

[2] X. Zhang, L. Chen, R. Orenstein, X. Lu, C. Wang, M. Yanilmaz, M. Peng, Y. Dong, Y. Liu and X. Zhang, *Energy Storage Mater.*, 2024, **70**,103500.

[3] H. Liu, Z. Xin, B. Cao, Z. Xu, B. Xu, Q. Zhu, J. L. Yang, B. Zhang and H. J. Fan, *Adv. Funct. Mater.*, 2023, **34**, 2309840.

[4] J. Zhang, C. Zhou, Y. Xie, Q. Nan, Y. Gao, F. Li, P. Rao, J. Li, X. Tian and X. Shi, *Small*, 2024, **20**, 2404237.

[5] Z. Hu, F. Zhang, A. Zhou, X. Hu, Q. Yan, Y. Liu, F. Arshad, Z. Li, R. Chen, F. Wu, L. Li, *Nano-Micro Lett.*, 2023, **15**, 171.

[6] R. Chen, W. Zhang, Q. Huang, C. Guan, W. Zong, Y. Dai, Z. Du, Z. Zhang, J. Li, F. Guo, X. Gao, H. Dong, J. Zhu, X. Wang, G. He, *Nano-Micro Lett.*, 2023, **15**, 81.

[7] X. Yan, Y. Tong, Y. Liu, X. Li, Z. Qin, Z. Wu, W. Hu, *Nanomaterials*, 2023, **13**, 1547.

[8] G. Zhang, J. Zhu, K. Wang, Q. Li, W. Fu, X.-X. Liu and X. Sun, *Chem. Commun.*, 2024, **60**, 1317-1320.

[9] J. Chen, S. Li, F. Li, W. Sun, Z. Nie, B. Xiao, Y. Cheng, X. Xu, *ACS Appl. Mater. Interfaces*, 2024, **16**, 42153-42163.

[10] L. Zhou, W. Zhou, H. Wang, Q. Deng, X. Ai, X.-X. Zeng, X. Wu, C. Zhou, W. Ling, *Chem. Eng. J.*, 2024, **492**, 152324.

[11] G. Zhang, J. Zhu, K. Wang, Q. Li, W. Fu, X.-X. Liu, X. Sun, *Chem. Commun.*, 2024, **60**, 1317-1320.

[12] L. Wang, P.P. Wang, H.Q. Zhou, Z.B. Wang and C.Y. Xu, *Nano Energy*, 2024, **119**, 109076.

[13] Y. Xiong, Q. Li, K. Luo, L. Zhong, G. Li, S. Zhong and D. Yan, *J. Energy Storage*, 2023, **68**, 107655.

[14] H. Liu, H. Deng, S. Liu, Y. Hou, S. Wang, S. Liang, T. Xu, Q. Shen, S. Li, J. Qiu, *ACS Appl. Mater. Interfaces*, 2024, **16**, 35217-35224.